

# RECENT RESULTS FROM ULTRA-HIGH ENERGY COSMIC RAY EXPERIMENTS WITH IMPACT ON HADRONIC INTERACTION MODELS

H.P. DEMBINSKI<sup>1</sup>, for the Pierre Auger Collaboration<sup>2</sup>

<sup>1</sup>*IKP, Karlsruhe Institute of Technology (KIT), Postfach 3640, D-76021 Karlsruhe, Germany*

<sup>2</sup>*Observatorio Pierre Auger, Av. San Martín Norte 304, 5613 Malargüe, Argentina*

(Full author list: [http://www.auger.org/archive/authors\\_2011\\_12.html](http://www.auger.org/archive/authors_2011_12.html))

Cosmic rays are nuclei with a wide mass and energy spectrum, the latter spanning over 11 orders of magnitude. A small fraction of cosmic rays reach ultra-high energies greater than  $10^{18}$  eV. If such cosmic rays interact with the nuclei in Earth's atmosphere, centre-of-mass energies of the order of ten to hundred TeV are reached. Therefore they can be used to challenge our understanding of hadronic interactions at energies far beyond the reach of man-made colliders. We present recent measurements from the Pierre Auger Observatory, Telescope Array, and HiRes, sensitive to cosmic ray mass and hadronic interaction models. We highlight the measurements of the proton-air cross-section and of a muon deficit in contemporary hadronic interaction models.

## 1 Introduction

The cosmic ray flux above  $10^{18}$  eV drops below one particle per  $\text{km}^2$  and year and therefore suitable detectors need a huge aperture. This is achieved by exploiting extensive air showers induced by the cosmic rays in Earth's atmosphere, which effectively acts as a calorimeter. The calorimeter is read out using two techniques: sparse ground arrays of particle detectors and fluorescence telescopes.

A surface detector array (SD) catches the tail of the air shower that reaches the ground and samples its lateral density profile. The density drops rapidly as a function of radial distance to the shower axis, but can still be measured up to several kilometres away, which enables experiments to use sparse grids with large spacings.

A fluorescence detector (FD) exploits that a part of the ionization energy deposited by charged particles in air is converted and isotropically emitted as UV light. In dark moonless nights, the longitudinal development of the shower can be tracked with telescopes using fast PMT cameras up to distances of several tens of kilometres. The fluorescence yield in air of about five photons per MeV energy deposit has been measured in the laboratory<sup>1</sup> and therefore it is possible to reconstruct the total energy of the cosmic ray initiating the shower by integrating the observed energy losses, while correcting only for a small fraction of about 10 % to 20 % of "invisible" energy carried by high-energy muons and neutrinos<sup>2</sup>.

These experimental techniques are very successful, but it is difficult to extract information about hadronic interactions from air shower measurements mainly due to two unknowns. The first unknown is the mass composition of cosmic rays, an interesting topic on its own. The other unknown concerns the shower development, which has to be modelled since the first interaction itself cannot be observed directly. Since all observables sensitive to hadronic interaction prop-

erties also depend on the mass of the cosmic ray, there is always an interplay between the two. A separation of the influences of mass and hadronic interaction properties requires a combined study of at least two observables or a selection of a proton-pure sample.

Hybrid detectors combining a SD and FD offer more observables and thus are best for these studies. We will concentrate in this article on measurements of the Pierre Auger Observatory<sup>3,4</sup>, Telescope Array<sup>5</sup>, and the HiRes observatory<sup>6</sup>. HiRes lacks a Surface Detector and Telescope Array is still in its early stage of data analysis, so that most of the recent results come from the Auger Observatory.

A brief overview of cosmic ray measurements related to astrophysics will be given in section 2, which will also serve to demonstrate the quality of the data. We will then discuss measurements of the depth  $X_{\max}$  of the maximum of longitudinal shower development in section 3, which is currently the main observable interpreted in terms of mass composition and hadronic interactions. The measurement of the proton-air cross section from the slope of the tail of the  $X_{\max}$ -distribution is a good example of how systematic uncertainties due to the unknown mass composition can be significantly reduced. We will highlight recent measurements in section 4. We conclude with the observation of an unexpectedly large ratio of the muon to the electromagnetic component in air showers in section 5.

## 2 Cosmic ray flux and sources

The cosmic ray flux measured at Earth contains information about the unknown sources of cosmic rays and propagation effects in the intergalactic medium. If cosmic rays are accelerated in distant astrophysical objects like active galactic nuclei, the GZK effect<sup>10</sup> should lead to a flux suppression<sup>11</sup> around  $6 \times 10^{19}$  eV, which was observed by HiRes<sup>12</sup>, but not by AGASA<sup>13</sup>. The flux suppression was then independently confirmed by the Auger Observatory<sup>14</sup>. Fig. 1 compares the most recent measurements of Auger and Telescope Array<sup>7,8,9</sup>. The shapes of the two spectra agree very well. The diagonal offset is consistent with the systematic uncertainties of the energy scales of the two experiments, which have a systematic uncertainty of 22 % and 21 %, respectively<sup>15,16</sup>.

Patterns in the almost isotropic distribution of arrival directions of cosmic rays at Earth shed light on the unknown sources and the physical origin. The Auger Collaboration reported a correlation of the arrival directions of cosmic rays at energies larger than  $5.7 \times 10^{19}$  eV with active galactic nuclei, which trace the population density of nearby galaxies<sup>17</sup>. So far this claim was neither conclusively confirmed nor ruled out by other experiments<sup>18</sup>.

## 3 Measurements of the shower development

Simple Heitler-type models and the (semi-)superposition model for the interaction of heavy nuclei describe some features of hadronic air showers well<sup>22,23</sup>. From this theoretical approach one can derive that the mean of the  $X_{\max}$ -distribution depends logarithmically on energy  $E$  and mass  $A$

$$\langle X_{\max} \rangle \approx D_p (\ln E - \langle \ln A \rangle) + c, \quad (1)$$

with elongation rate  $D_p = dX_{\max}/d \ln E$  that depends on the energy evolution of multiplicity and elasticity of the hadronic interaction, and parameter  $c$  that depends strongly on the proton-air cross-section and logarithmically on elasticity and multiplicity of the first interaction<sup>23</sup>. Since the function  $\langle \ln A \rangle(E)$  is unknown one cannot simply fit Eq. 1 to observations in order to learn about  $D_p$  and  $c$ .

The spread  $\sigma(X_{\max}) = \sqrt{\text{Var}(X_{\max})}$  of the  $X_{\max}$ -distribution carries further information about the mass composition and the cross-section of the first interaction. For proton showers,

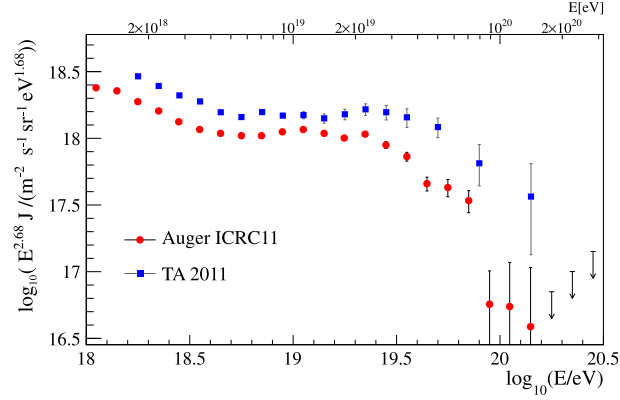


Figure 1: Flux  $J$  of cosmic rays in log-log scale as measured by the Auger Observatory and Telescope Array multiplied by  $E^{2.68}$  in order to emphasize the features.<sup>7,8,9</sup>

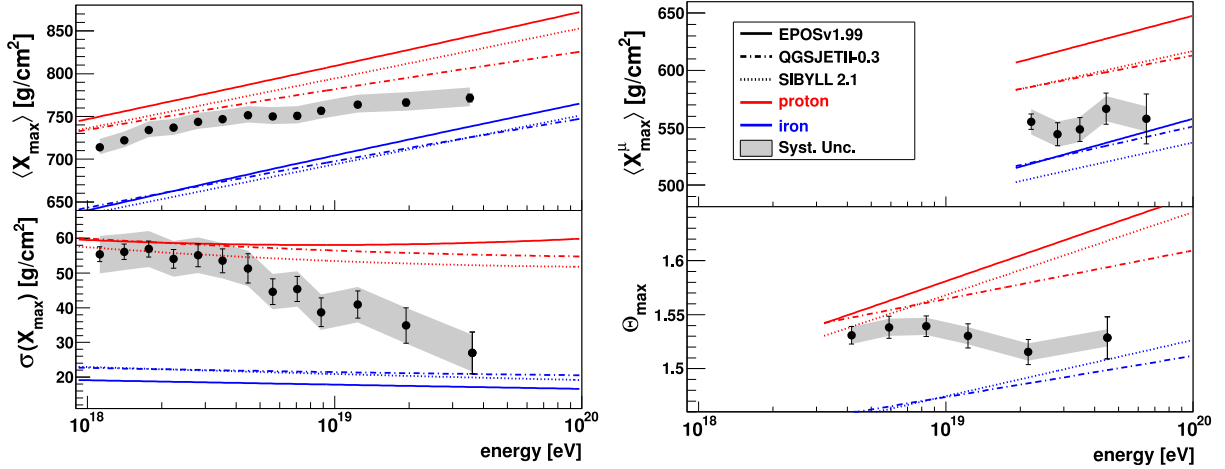


Figure 2: Left: Mean  $\langle X_{\max} \rangle$  and spread  $\sigma(X_{\max}) = \sqrt{\text{Var}(X_{\max})}$  of the depth of shower maximum as a function of energy. Compared are predictions from hadronic interaction models for proton and iron showers. Right: Mean production distance  $\langle X_{\max}^{\mu} \rangle$  of muons that reach ground and  $\Theta_{\max}$ , a measure of the shower inclination that maximises the circular asymmetry in signal risetime on the ground.<sup>19</sup>

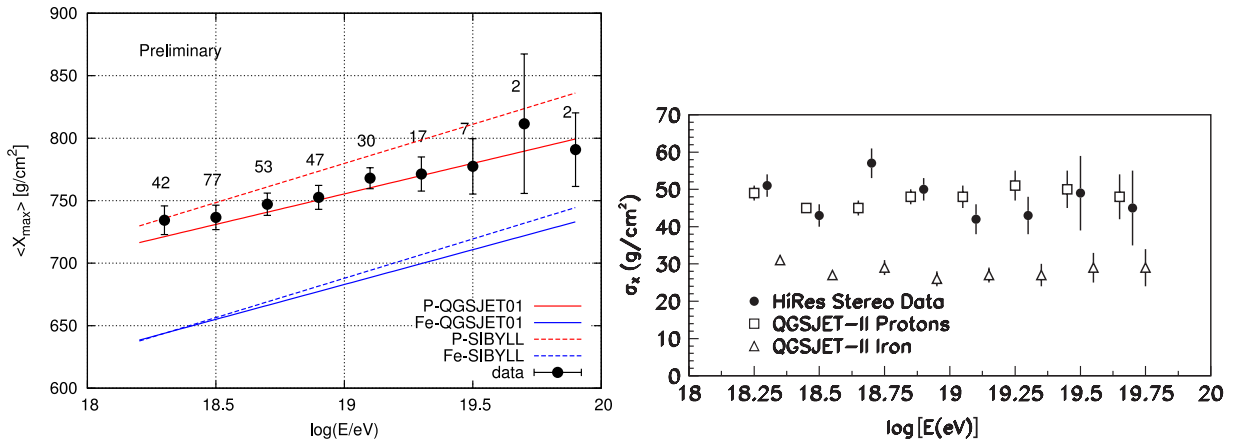


Figure 3: Left: Preliminary measurement of the mean depth  $\langle X_{\max} \rangle$  of shower maximum as a function of energy as measured by Telescope Array (preliminary). Compared are predictions from hadronic interaction models for proton and iron showers, as described in the text.<sup>20</sup> Right: Measurement of the fluctuations of the observed  $X_{\max}$ -distribution by HiRes as a function of energy. The fluctuation indicator  $\sigma_X$  is described in the text.<sup>21</sup>

one finds

$$\sigma^2(X_{\max}^p) = \lambda_{\text{int}}^2 + \sigma^2(\Delta X), \quad (2)$$

with the hadronic interaction length  $\lambda_{\text{int}}$  and shower development length  $\Delta X$ , the slant depth between the first interaction point and  $X_{\max}$ . In case of a mixed composition the situation becomes more complex and one finds

$$\sigma^2(X_{\max}) = \langle \sigma_i^2 \rangle + D_p^2 (\langle \ln^2 A \rangle - \langle \ln A \rangle^2), \quad (3)$$

where  $\sigma_i$  is the fluctuation of component  $i$ <sup>23</sup>. Due to the second term, a mixed composition can have larger  $X_{\max}$ -fluctuations than a proton-pure composition, which otherwise shows the largest fluctuations due to the large hadronic interaction length of protons.

Measurements of the mean and the fluctuations of  $X_{\max}$  from Auger, Telescope Array, and HiRes are shown in Fig. 2 and Fig. 3 and compared with predictions of hadronic interaction models<sup>19,20,21</sup>. The Auger Collaboration uses data-based cuts to ensure that the observed  $X_{\max}$ -distribution is not biased by the efficiency of the detector. Telescope Array and HiRes compare the biased  $X_{\max}$ -distribution with equally biased predictions from simulations. However, this approach is expected to break the linear relationship between  $\langle X_{\max} \rangle$  and  $\langle \ln A \rangle$  in Eq. 1. The fluctuation observable also differs between Auger and HiRes. While the Auger Collaboration uses the standard deviation of  $X_{\max}$  and subtracts the detector resolution, HiRes fits a Gaussian truncated at two standard deviations to the  $X_{\max}$ -distribution and reports its  $\sigma$ -parameter<sup>21</sup>.

The differences in the observables and energy scales make a quantitative comparison between Auger and Telescope Array/HiRes difficult. If the hadronic models described the interactions properly, the results of the Auger Observatory would indicate a transition from a light or mixed to a heavy mass composition between  $10^{18}$  eV and  $6 \times 10^{19}$  eV, while the results of Telescope Array/HiRes are compatible with a proton-pure scenario. However, heavier composition scenarios cannot be excluded either by Telescope Array/HiRes due to the still large uncertainties.

Since the FD has a limited duty cycle of about 10%, SD observables sensitive to the longitudinal shower development are also investigated. The Auger Collaboration has published measurements of the mean depth  $\langle X_{\max}^\mu \rangle$  of muon production and  $\Theta_{\max}$ , the logarithm of the zenith angle  $\theta$  at which the signal risetime asymmetry around the shower axis is at maximum<sup>19</sup>. The muon production depth  $X_{\max}^\mu$  is determined by tracking the space-time coordinates of muon signals back from the ground along their light-like paths to their production point on the shower axis. Both observables are strongly correlated with  $X_{\max}$ . These analyses also indicate an increasing faster shower development as the energy rises, compatible with the FD measurements. The challenge for hadronic interaction models is to describe all these observations consistently for a given mass composition assumption.

#### 4 Proton-air cross-section

The Auger Collaboration has recently presented a measurement of the inelastic proton-air cross-section  $\sigma_{\text{inel}}^{\text{p-air}}$  at a center-of-mass energy  $\sqrt{s} = 57$  TeV based on the exponential tail of the  $X_{\max}$ -distribution with an improved version of a method originally developed for the Fly's Eye experiment<sup>24,26</sup>.

The depth of the first interaction is exponentially distributed, which is reflected in the tail of the  $X_{\max}$ -distribution. The slope of the tail therefore strongly depends on the proton-air cross-section  $\sigma_{\text{inel}}^{\text{p-air}}$ . The mapping is derived from air shower simulations, using a consistent rescaling of the cross-section as a function of the center-of-mass energy. Systematic uncertainties with respect to the fluctuations of the shower development have only a weak effect on the slope of the tail. Moreover, the tail is proton-rich, since protons are the most deeply penetrating particles.

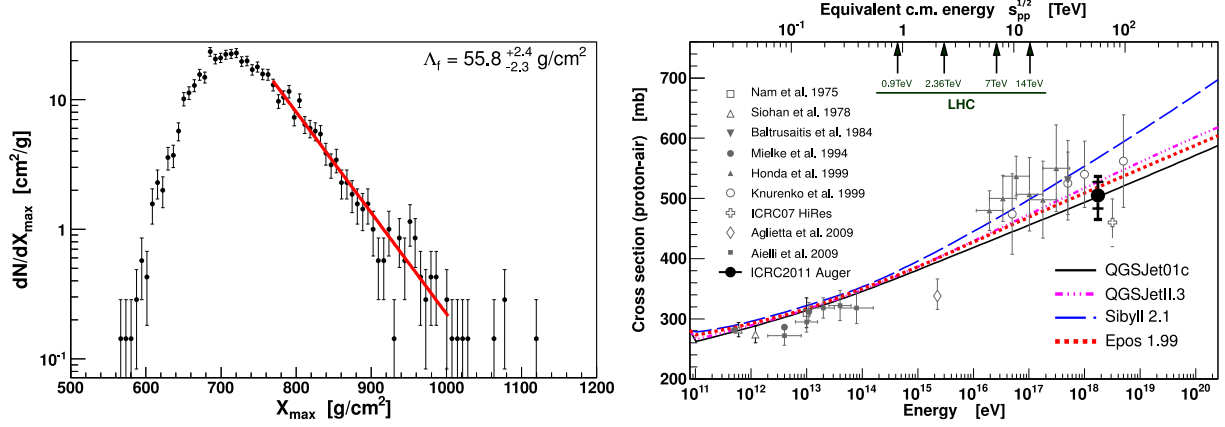


Figure 4: Left:  $X_{\max}$ -distribution in the energy range  $10^{18}$  to  $10^{18.5}$  eV measured by the Auger Observatory and fit of its exponential tail. Right: inelastic proton-air cross-section from Auger, HiRes, and other experiments. The plotted Auger and HiRes results are based on the assumption of a negligible helium flux.<sup>24,25</sup>

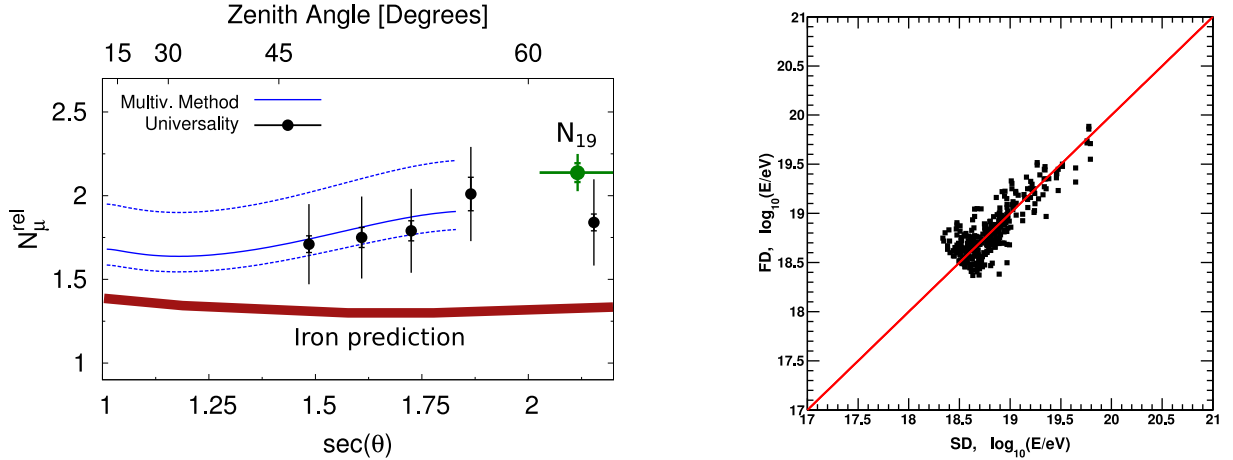


Figure 5: Left: Relative muon density  $N_{\mu}^{\text{rel}}$  at a radial distance of 1000 m at  $10^{19}$  eV with respect to QGSJET-II predictions for proton showers as measured by the Auger Observatory. Shown are the muon counting method, shower universality method, and the  $N_{19}$  method based on very inclined showers. Also given is the prediction for a pure iron composition.<sup>28,29</sup> Right: Correlation of the SD energy  $E_{SD}$ , calibrated via Monte-Carlo simulation of the detector response, and the FD energy  $E_{FD}$  measured by Telescope Array. The SD energy  $E_{SD}$  was rescaled by the factor  $\langle E_{FD}/E_{SD} \rangle = 1/1.27$  to shift the points onto the diagonal line.<sup>16</sup>

The analysis would be harmed by a large fraction of helium or photons in the data, which contribute to the tail. The Auger Collaboration has published tight bounds on the photon-fraction<sup>27</sup>, but there are no limits on the helium fraction. Therefore, the proton-air cross-section is a conditional statement. Assuming that the helium contribution is negligible between  $10^{18}$  eV and  $10^{18.5}$  eV, the inelastic proton-air cross-section at  $\sqrt{s} = 57$  TeV from the Auger analysis<sup>24</sup> is

$$\sigma_{\text{inel}}^{\text{p-air}} = (505 \pm 22_{\text{stat}} \text{ } ^{+20}_{-15}_{\text{sys}}) \text{ mb}, \quad (4)$$

as shown Fig. 4. The older HiRes-result  $\sigma_{\text{inel}}^{\text{p-air}} = 460 \pm 14_{\text{stat}} \text{ } ^{+39}_{-26}_{\text{sys}} \text{ mb}$  is one sigma smaller<sup>25</sup>. If half of the events were helium, these estimates would have to be reduced by 80 mb.

## 5 Muon deficit in simulations

The ratio of photons and electrons produced in an air shower on the one hand (electromagnetic component) and muons on the other hand (muon component) can be predicted with air shower

simulation codes and measured with hybrid detectors. A straightforward way is to use very inclined showers. At zenith angles larger than  $60^\circ$ , the mass overburden of the atmosphere is so large that only the penetrating muon component reaches the ground. Simultaneously, the FD measurement of the shower energy is based on the electromagnetic component and thus FD energy estimator and the SD shower size estimator for an inclined shower yields the ratio. The Auger Collaboration uses this method ( $N_{19}$  method) and several others which also work at lower zenith angles<sup>28,29</sup> and finds a large muon deficit in simulations. A compilation is shown on the left hand side of Fig. 5.

Telescope Array has not yet analysed its data in this fashion, but reports a mismatch between the energy scale of the SD established with Monte-Carlo simulation of the detector response and the energy scale of the FD<sup>16</sup>, shown on the right hand side of Fig. 5. In order to get both in agreement, the SD energy is rescaled by a factor of  $\langle E_{FD}/E_{SD} \rangle = 1/1.27$ . The origin of this mismatch is currently under investigation, but a lack of muons in simulations is a possible explanation.

## Acknowledgments

We are indebted to M. Unger and C. Dobrigkeit for valuable comments on this article.

## References

1. J. Rosado *et al.* in *Proc. 32nd ICRC* (Beijing, China, 2011).
2. H.M.J. Barbosa *et al.*, *Astropart. Phys.* **22**, 159–166 (2004).
3. I. Allekotte *et al.* (Pierre Auger Collab.), *Nucl. Instrum. Meth.* **A 586**, 409–420 (2007).
4. J. Abraham *et al.* (Pierre Auger Collab.), *Nucl. Instrum. Meth.* **A 620**, 227–251 (2010).
5. T. Nonaka *et al.* (Telescope Array Collab.) in *Proc. 32nd ICRC* (Beijing, China, 2011).
6. J.H. Boyer *et al.*, *Nucl. Instrum. Meth.* **A 482**, 457 (2002).
7. M. Unger, rapporteur talk at *Proc. 32nd ICRC* (Beijing, China, 2011).
8. F. Salamida *et al.* (Pierre Auger Collab.) in *Proc. 32nd ICRC* (Beijing, China, 2011), arXiv:1107.4809v1; J. Abraham *et al.* (Pierre Auger Collab.), *Phys. Lett. B* **685**, 239–246 (2010).
9. Y. Tsunesada *et al.* (Telescope Array Collab.) in *Proc. 32nd ICRC* (Beijing, China, 2011).
10. K. Greisen, *Phys. Rev. Lett.* **16**, 748–750; G.T. Zatsepin and V.A. Kuz'min, *JETP Lett.* **4**, 78–80 (1966).
11. V.S. Berezinsky and S.I. Grigorieva, *Astron. Astrophys.* **199**, 1 (1988).
12. R.U. Abbasi *et al.* (HiRes Collab.), *Phys. Rev. Lett.* **100**, 101101 (2008).
13. N. Sakaki *et al.* (AGASA Collab.) in *Proc. 27th ICRC* (Hamburg, Germany, 2001).
14. J. Abraham *et al.* (Pierre Auger Collab.), *Phys. Rev. Lett.* **101**, 061101 (2008).
15. R. Pesce *et al.* (Pierre Auger Collab.) in *Proc. 32nd ICRC* (Beijing, China, 2011), arXiv:1107.4809v1.
16. T. Abu-Zayyad *et al.* (Telescope Array Collab.) in *Proc. 32nd ICRC* (Beijing, China, 2011).
17. P. Abreu *et al.* (Pierre Auger Collab.), *Astropart. Phys.* **34**, 314–326 (2010).
18. I. Tkachev *et al.* (Telescope Array Collab.) in *Proc. 32nd ICRC* (Beijing, China, 2011).
19. D. Garcia-Pinto *et al.* (Pierre Auger Collab.) in *Proc. 32nd ICRC* (Beijing, China, 2011), arXiv:1107.4804v1; J. Abraham *et al.* (Pierre Auger Collab.), *Phys. Rev. Lett.* **104**, 091101 (2010).
20. Y. Tameda *et al.* (Telescope Array Collab.) in *Proc. 32nd ICRC* (Beijing, China, 2011).
21. R.U. Abbasi *et al.* (HiRes Collab.), *Phys. Rev. Lett.* **104**, 161101 (2010).
22. J. Matthews, *Astropart. Phys.* **22**, 387–397 (2005).
23. K.-H. Kampert and M. Unger, arXiv:1201.0018 (2012).
24. R. Ulrich *et al.* (Pierre Auger Collab.) in *Proc. 32nd ICRC* (Beijing, China, 2011), arXiv:1107.4804v1.
25. K. Belov *et al.* (HiRes Collab.) in *Proc. 30th ICRC* (Mérida, Mexico, 2007).
26. R.W. Ellsworth *et al.*, *Phys. Rev. D* **26**, 336–339 (1982).
27. M. Settimo *et al.* (Pierre Auger Collab.) in *Proc. 32nd ICRC* (Beijing, China, 2011), arXiv:1107.4805v1.
28. J. Allen *et al.* (Pierre Auger Collab.) in *Proc. 32nd ICRC* (Beijing, China, 2011), arXiv:1107.4804v1.
29. G. Rodriguez *et al.* (Pierre Auger Collab.) in *Proc. 32nd ICRC* (Beijing, China, 2011), arXiv:1107.4809v1.